[23] Y. Chang, J. J. Teo, H. C. Zeng, *Langmuir* **2005**, *21*, 1074.
[24] D. Snoke, *Science* **2002**, *298*, 1368.
[25] P. McFadyen, E. Matijevic, *J. Colloid Interface Sci.* **1973**, *44*, 95.
[26] D. Wang, M. Mo, D. Yu, L. Xu, F. Li, Y. Qian, *Cryst. Growth Des.* **2003**, *3*, 717.
[27] Y. Chang, H. C. Zeng, *Cryst. Growth Des.* **2004**, *4*, 273.
[28] a) M. J. Siegfried, K.-S. Choi, *Adv. Mater.* **2004**, *16*, 1743. b) M. J. Siegfried, K.-S. Choi, *Angew. Chem. Int. Ed.* **2005**, *44*, 3218.
[29] W. Wang, G. Wang, X. Wang, Y. Zhan, Y. Liu, C. Zheng, *Adv. Mater.* **2002**, *14*, 67.
[30] L. Gou, C. J. Murphy, *Nano Lett.* **2003**, *3*, 231.
[31] R. Liu, F. Oba, E. W. Bohannan, F. Ernst, J. A. Switzer, *Chem. Mater.* **2003**, *15*, 4882.
[32] P. He, X. Shen, H. Gao, *J. Colloid Interface Sci.* **2005**, *284*, 510.
[33] Z. Wang, X. Chen, J. Liu, M. Mo, L. Yang, Y. Qian, *Solid State Commun.* **2004**, *130*, 585.
[34] G. H. Yang, E. T. Kang, K. G. Neoh, Y. Zhang, K. L. Tan, *Langmuir* **2001**, *17*, 211.
[35] W. Prissanaroon, N. Brack, P. J. Pigram, P. Hale, P. Kappen, J. Liesegang, *Thin Solid Films* **2005**, *477*, 131.
[36] J. F. Moulder, W. F. Stickle, P. E. Sobol, K. D. Bomben, *Handbook of X-ray Photoelectron Spectroscopy*, Perkin-Elmer Corporation Physical Electronics Division, Eden Prairie, MN **1992**.

Photoembossing of Periodic Relief Structures Using Polymerization-Induced Diffusion: A Combinatorial Study**

By *Carlos Sánchez*, *Berend-Jan de Gans*, *Dimitri Kozodaev*, *Alexander Alexeev*, *Michael J. Escuti*, *Chris van Heesch*, *Thijs Bel*, *Ulrich S. Schubert*, *Cees W. M. Bastiaansen*,* and *Dirk J. Broer*

Polymeric relief microstructures are extensively used in biosensors, cell-growth arrays, and as microelectronic and microoptical elements in displays.[1–4] To generate these structures, replication methods based on physical contact are used, like embossing or cast-molding. In case of embossing, relief features are transferred by pressing a polymer film against a microstructured rigid master.[5,6] Cast-molding uses a polymer precursor that is poured onto a master, cured, and released to obtain an inverse replica.[7] Relief microstructures can also be made by lithography via a light-induced solubility change of a polymeric photoresist.[8] A wet-etching step develops the final relief structure. Recently, a new solvent-free photolithographic technique was proposed to prepare surface-relief structures.[9–11] The process that we will refer to as "photoembossing" is schematically shown in Figure 1. A photopolymer blend comprising a polymeric binder, a multireactive acrylate, and a photoinitiator is processed as a solid thin film onto a substrate. An irradiation step through a lithographic mask at room temperature (RT) generates radicals in the exposed areas. The photopolymer blend is glassy at RT, which allows the use of contact masks. Monomer diffusion and polymerization are inhibited at this stage, and a free-radical latent image of the mask is formed. A subsequent heating step enhances monomer mobility and polymerization in the irradiated areas. Consumption of monomer in these regions leads to a net flux of unreacted monomer from the unexposed to the exposed areas, resulting in a surface deformation whose final shape is determined by diffusion and surface tension. Photoembossing does not involve any wet developing step, and the mask can directly contact the photopolymer. Therefore, photoembossing is also very attractive from an industrial standpoint.[11]

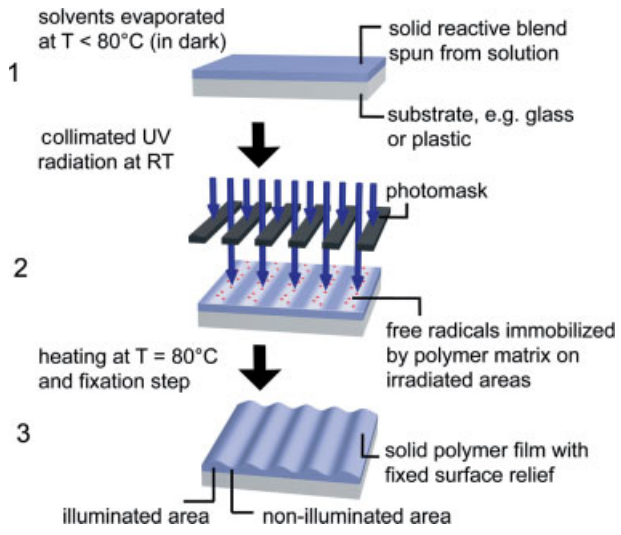

Figure 1. Schematic representation of the photoembossing process. RT, room temperature.

A large variety of processing parameters influence the height and shape of the final relief structure, which determine its performance in specific applications. In this paper, we report on a combinatorial study on the influence of the structure period, energy dose, development temperature, film thickness, and photopolymer blend composition. Automated atomic force microscopy (AFM) is used to characterize the topography of the relief structures with high reproducibility and com-

[*] Dr. C. W. M. Bastiaansen, Dr. C. Sánchez, Dr. B.-J. de Gans, Dr. D. Kozodaev, Dr. A. Alexeev, Dr. M. J. Escuti, C. van Heesch, Prof. U. S. Schubert, Prof. D. J. Broer
Eindhoven University of Technology, Dutch Polymer Institute (DPI)
P.O. Box 902, NL-5600 AX Eindhoven (The Netherlands)
E-mail: c.w.m.bastiaansen@tue.nl
T. Bel, Prof. D. J. Broer
Philips Research Laboratories
Prof. Holstlaan 4, NL-5656 AA Eindhoven (The Netherlands)

[**] The research of Carlos Sánchez, Berend-Jan de Gans, Dimitri Kozodaev, Alexander Alexeev, Michael J. Escuti, Chris van Heesch, Ulrich S. Schubert, Cees W. M. Bastiaansen, and Dirk J. Broer forms part of the research program of the Dutch Polymer Institute (DPI).

 DOI: 10.1002/adma.200500777

ADVANCED MATERIALS

parability. Besides the basic insight provided by our combinatorial methodology, we show its technological impact for the rapid identification of the conditions for which a certain structure is obtained.

A typical photopolymer blend comprises a 1:1 ratio of poly(benzyl methacrylate) as binder and multifunctional acrylate (dipentaerythritol penta-/hexa-acrylate), plus a small percentage of radical photoinitiator. We first generated a two-dimensional library in which the period of the grating structure (Λ) and the energy dose (E) were systematically varied over its two axes. To introduce a variation of the period over one axis, we used a lithographic line mask with four different grating periods. The energy dose was varied with a linear variable neutral density filter with the optical density (OD) ranging from 0.04 (no absorption) to 2 in eleven steps. The filter was put on top of the mask with the OD steps varying perpendicular to the variation of the period of the lithographic mask. We then irradiated the photopolymer film for 10 min using a lithographic exposure system. Filter and mask were then removed, and the film was heated on a heating stage at 80 °C for an additional 10 min. This creates a library of 44 different samples (4 different rows of different periods and 11 columns of different energy doses, as shown in Fig. 2a). Flood-exposing (10 min) and subsequent heating at 80 °C (10 min) fixes the sample. The relief height (taken as the difference in vertical distance between the central part of the irradiated and non-irradiated area) was measured by automated AFM.

Figure 2b shows the results as a function of energy dose and period. The optimum energy dose is reached at lower doses for larger periods. The optimum is not reached for the 5 μm pitch (or period) in the range of energies we studied. Figure 2c shows relief profiles corresponding to the 40 μm period gratings obtained with increasing energy doses. For small energy doses, the relief profile is a sinusoid with small amplitude. As the energy dose increases, an optimum height of 450 nm is obtained while maintaining the sinusoidal shape (AFM image in Fig. 2c, inset). For doses higher than the optimum, the amplitude decreases again, and two peaks appear at the edges of the exposed areas.

This phenomenology can be explained by the diffusion-polymerization model proposed for this process by Leewis et al.[12,13] According to this model, the polymerization-induced monomer-concentration gradient together with diffusivity differences, crosslinking properties, interaction between the different components, and the surface free energy determine the migration of monomer and therefore the final relief structure. In our case, irradiation generates radicals that are immobile at RT, just like the monomer, due to the glassy nature of the photopolymer blend. Heating enhances mobility. Polymerization then occurs selectively in the irradiated areas, generating a composition gradient that triggers the diffusion process. In addition, local shrinkage in the bright areas due to network formation could favor the generation of free volume in these areas, enhancing diffusion.[10] At sub-optimal energy doses, only a small fraction of photoinitiator is activated, resulting in low conversion and therefore low structure heights. Higher doses enhance the swelling of the exposed areas and therefore increase the relief height, while surface tension determines the final features. An optimum between the diffusion and the polymerization processes is found in these conditions. For overexposed samples (above the optimum), monomer cannot reach the central part of the irradiated area as diffusion is strongly hindered by the high crosslinking density that is the result of the high radical concentration. Instead, the diffusing monomer reacts mainly at the edges of the exposed area, re-

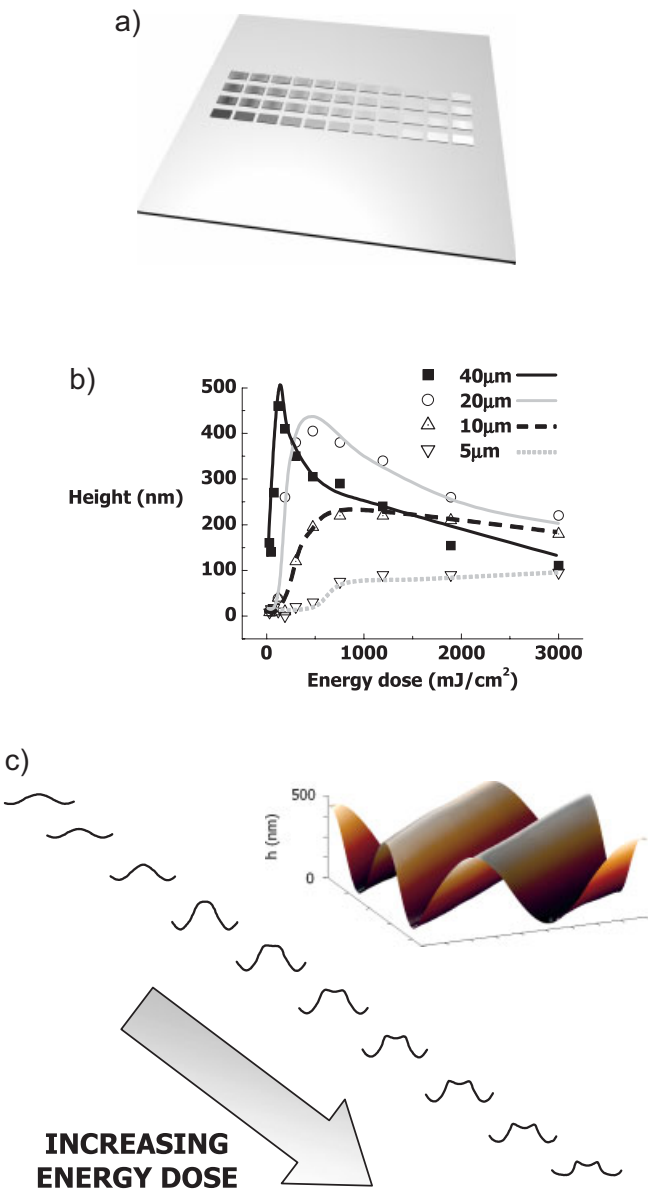

Figure 2. a) Schematic representation of a two-dimensional library of photoembossed samples. b) Relief height as a function of energy dose for different periods (lines are drawn to guide the eye). c) Surface-relief topographies of the 40 μm period samples for different energy doses, and typical AFM image of a photoembossed sample (inset).

sulting in the observed peaks. In this case, the balance between the diffusion and polymerization kinetics is in favor of polymerization. The same shape trend is observed as the period decreases. However, as mentioned previously, the optimum height is observed at higher energy doses for these smaller periods. Since the lateral dimensions are smaller, the appearance of the side shoulders requires higher degrees of crosslinking to hinder monomer diffusion to the central part of the exposed area and to produce accumulation of material in the lateral side of the exposed area. This shows that the typical diffusion length of monomer is within the range of the period of the structures and can be accurately controlled by the degree of curing. Note also the lower relief heights (at the optimum dose) obtained for smaller pitches. The energetic cost derived from the generation of new surface area[10] could explain this, since a decrease of the pitch keeping the same height would lead to the generation of more surface, which is expensive in terms of energy.

We also generated combinatorial libraries by varying the period Λ and the temperature (T) during baking. The same mask was used for lithographic exposure (10 min), keeping the light intensity constant. A temperature-gradient stage was used to heat the sample (10 min). Figure 3 shows the relief height obtained from two different libraries that cover processing temperatures from 50 to 135 °C. Relief height increases with temperature for the 40 μm and 20 μm periods. For smaller periods, an optimum temperature is obtained that decreases with period. We expected larger diffusivities of the monomer at high temperature, favoring the net flux of material. However, a too-high mobility could also result in (unwanted) migration of radicals to the non-irradiated areas, diminishing the driving force for monomer diffusion and thus relief height. This effect is more noticeable for the smaller periods. Topographic analysis shows the peaks at the edges of the irradiated areas (of the 40 μm pitch samples) disappearing at higher temperatures and possessing a more rounded shape. Again, enhanced monomer diffusion at higher temperatures explains this shape trend that is also observed for the 20 μm pitch samples.

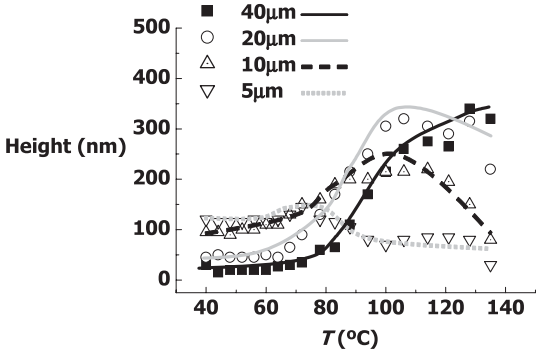

Figure 3. Relief height as a function of baking temperature for different periods.

We created libraries with discrete variations in period and thickness, consisting of arrays of cast films of different amounts of photopolymer blend. We used a chemically patterned substrate, consisting of an array of hydrophilic rectangles of 8.5 mm × 4.3 mm each, arranged in 11 columns and 4 rows, and surrounded by hydrophobic barriers.[14] When dispensing a sample, the liquid wets the hydrophilic area up to the hydrophobic barriers. The dried films have thicknesses ranging from 7 to 17 μm. Each column has similar thickness (±1 μm). To induce different periods, we exposed (10 min) through the lithographic mask and subsequently heated the array at 80 °C (10 min). Figure 4 shows the height of the resulting structures as a function of thickness. It is shown that

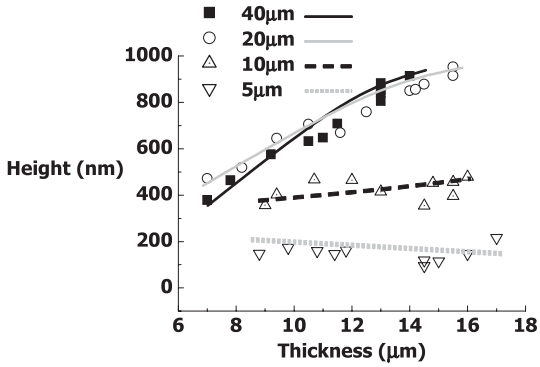

Figure 4. Relief height as a function of film thickness for different periods.

higher-relief heights are obtained in thicker films for the large pitches since more monomer is able to participate in the process. Analysis of the shape did not show a distinct correlation with thickness. No significant influence was observed in both height and shape for the smaller pitches. This shows that, in this regime, material throughout the thickness of the photopolymer is not contributing to the relief formation to the same extent. The lower layers of the photopolymer have a minor influence on the relief generation when the lateral dimensions are similar to the thickness of the film.

We also generated libraries varying the photopolymer composition and period. To this end, we used the same chemically patterned substrates on which we had cast films of different blends. The dried films had a thickness of about 7 μm (±1 μm). Each column had the same composition. The different periods were induced by exposing (10 min) the sample through the lithographic mask and subsequently heating it at 80 °C (10 min). Figure 5a shows the relief height of a sample in which the ratio of monomer to polymer is varied in discrete steps over one axis of the sample (5 wt.-% photoinitiator). Higher amounts of monomer give rise to higher relief heights. Prior to polymerization, samples with lower binder content were slightly tacky and appeared turbid, which indicates (par-

ADVANCED MATERIALS

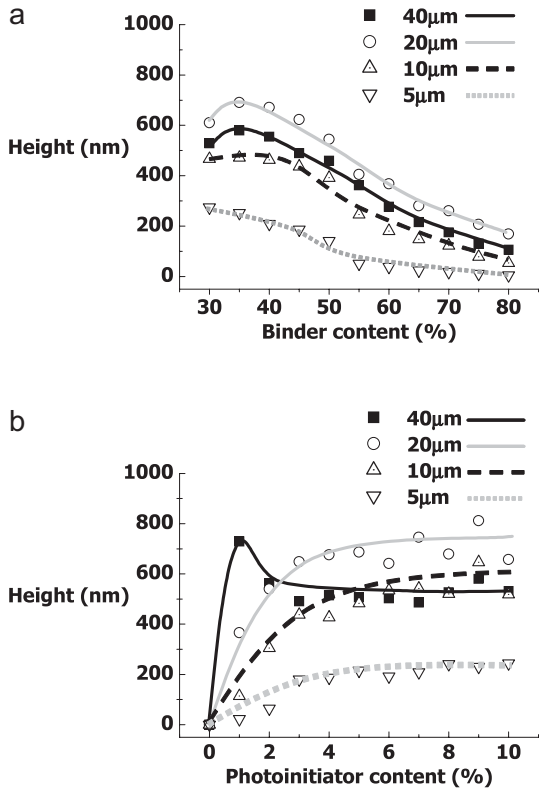

Figure 5. Relief height as a function of a) binder content and b) photoinitiator content for different periods.

tial) phase separation. Also, the relief structures were already partially developed just after irradiation prior to thermal development. A high monomer content decreases the glass-transition temperature and increases monomer mobility at RT. For applications this is undesirable, as the system becomes unsuitable for contact masking and for the generation of complex structures through multiple exposure steps.[11] The observed trend can also be understood within the framework of the previously mentioned diffusion-polymerization model.[12,13] As the monomer content decreases, the amount of material able to participate in the polymerization-diffusion process decreases as well. Together with a decreasing diffusivity due to a less-plasticized matrix, this inhibits the formation of higher-relief structures in the high-binder-content samples.

Figure 5b shows the relief height as a function of photoinitiator concentration (ranging from 0 to 10 % by weight, polymer/monomer mass ratio 1:1). For the 40 μm pitch, an optimum relief height is obtained at low photoinitiator concentration (1 %).[15] At higher concentrations, the relief height decreases again. Analysis of the relief shape shows that a nearly sinusoidal profile is obtained for these optimum conditions, whereas at higher concentrations shoulders begin to appear. For smaller pitches, the relief height increases with increasing photoinitiator content, although this trend is less marked for smaller pitches. Shape analysis of the 20 μm pitch samples reveals shoulders appearing at the highest photoinitiator content, while these are absent for smaller periods. These results are qualitatively identical to those found for the energy-dose pitch library. In both cases, we have a library with a gradient in radical concentration. In both cases, we find an optimum radical concentration that gives rise to a nearly sinusoidal profile with optimum height. Above this optimum concentration, the high crosslinking density hinders the diffusion of monomer to the central part of the exposed areas, resulting in lower heights and the appearance of shoulders in the edges of the exposed areas.

In conclusion, we developed a combinatorial methodology to create and evaluate libraries of photoembossed structures with systematic variations of the period of the structure, the energy dose, developing temperature, layer thickness, and composition of the photopolymer blend. The libraries are characterized using automated AFM, providing direct insight into the topography of the surface-relief structure. Optimum conditions to generate specific structures were easily identified. This combinatorial approach improves our understanding of surface-relief formation in these systems. In addition, we have a versatile tool to optimize the shape and height of polymeric structures of great interest in technological applications. This combinatorial methodology can easily be adapted to other, equally important systems, such as photoresists for microelectronic and photonic applications.

Experimental

To generate a variation of the period over one axis of a library we used a rectangular lithographic mask (101 mm × 20 mm) divided in four different sectors (101 mm × 5 mm), each of them consisting of transparent and dark lines with a periodicity of 40, 20, 10, and 5 μm. To induce an energy dose variation, we used a linear variable neutral-density filter (rectangular shape: 101 mm × 25 mm) increasing from optical density (*OD*) 0.04 (no absorption) to 2 in eleven steps (9 mm × 25 mm) of 0.2. A temperature-gradient heating stage (Leica VM HB) was employed to generate the temperature–period libraries. The stage has a gradient of T ranging from 50 to 260 °C over a distance of 30 cm. The length of our exposed area was about 10 cm; therefore, a range of about 60–70 °C could be covered with a single library. To generate libraries with composition and thickness variations, we employed a substrate that was chemically patterned with an array of rectangles (8.5 mm × 4.3 mm) arranged in 11 columns and 4 rows (same dimensions as the sectors obtained in the energy–period libraries). Rectangles were hydrophilic while the outer part was hydrophobic. To create these substrates, clean glass plates were coated with a negative photoresist that was subsequently exposed through a stainless-steel mask with rectangular holes corresponding to the sectors. After development, the substrate was coated with a fluorinated silane ((tridecafluoro-1,1,2,2-tetrahydrooctyl)-1-trichlorosilane) [16]. Finally, the resist was stripped, leaving the sectors hydrophilic while the surrounding area was fluorinated.

We prepared blends of poly(benzyl methacrylate) (Scientific Polymer Products, weight-average molecular weight (M_w) 70 000 g mol^{-1}) and dipentaerythritol penta-/hexa-acrylate (Aldrich) in a mass ratio 1:1, plus 5 wt.-% of Irgacure 369 photoinitiator (Ciba), for the energy dose–period and temperature–period libraries. We obtained films (2.6 μm thick) by spin-coating solutions in propylene glycol monomethyl ether acetate on square glass substrates (150 mm × 150 mm, D263 grade). A polymer/monomer mixture (1:1 w/w) with 5 % of photoinitiator by weight was dissolved in a mixture of isopropyl ace-

tate and methyl benzoate (90:10 w/w) and used for the thickness–period library. Different amounts of this mixture were dispensed using a micropipette (Brand Transferpette) in the different columns. Solvent was evaporated under ambient conditions. Thicknesses were characterized using a stylus profilometer (Dektak 3M). The same mixture of solvents was used for the composition–period libraries.

The exposure was performed using an USHIO lithographic system (filter at 365 nm, intensity 5 mW cm^{-2}). After exposure and heating, all the samples were fully polymerized by flood exposure for 10 min and heating at 80 °C for an additional 10 min to fix the relief structure. We checked that this step had a minor influence on the final relief structure. The topography was measured using an automated atomic force microscope (NT-MDT Solver P7 LS, Moscow, Russia) with a motorized Yθ-stage. The stage moves automatically to the 44 programmed coordinates on the sample surface corresponding to different processing conditions (e.g., energy–period, temperature–period). In case of the temperature–period library, the sample was virtually divided into 44 samples (11 × 4) and temperatures were estimated using a contact thermometer. All samples were prepared in a clean room (class 100).

Received: April 17, 2005
Final version: June 29, 2005
Published online: September 15, 2005

[1] K. Y. Suh, J. Seong, A. Khademhosseini, P. E. Laibinis, R. Langer, *Biomaterials* **2004**, *25*, 557.
[2] N. Stutzmann, R. H. Friend, H. Sirringhaus, *Science* **2003**, *299*, 1881.
[3] C. Kim, P. E. Burrows, S. R. Forrest, *Science* **2000**, *288*, 831.
[4] O. J. A. Schueller, D. C. Duffy, J. A. Rogers, *Sens. Actuators, A* **1999**, *78*, 149.
[5] N. Stutzmann, T. A. Tervoort, C. W. M. Bastiaansen, K. Feldman, P. Smith, *Adv. Mater.* **2000**, *12*, 557.
[6] G. Fichet, N. Stutzmann, B. V. O. Muir, W. T. S. Huck, *Adv. Mater.* **2002**, *14*, 47.
[7] E. Kim, Y. N. Xia, G. M. Whitesides, *Nature* **1995**, *376*, 581.
[8] H. J. Levinson, *Principles of Lithography*, SPIE, Bellingham, WA **2001**.
[9] C. Croutxé-Barghorn, D. J. Lougnot, *Pure Appl. Opt.* **1996**, *5*, 811.
[10] O. Sakhno, T. Smirnova, *Optik* **2002**, *113*, 130.
[11] C. Witz, C. Sánchez, C. Bastiaansen, D. J. Broer, in *Handbook of Polymer Reaction Engineering*, Vol. 2 (Eds: T. Meyer, J. Keurentjes), Wiley-VCH, Weinheim, Germany **2005**, Ch. 19.
[12] C. M. Leewis, A. M. de Jong, L. J. van IJzendoorn, D. J. Broer, *J. Appl. Phys.* **2004**, *95*, 4125.
[13] C. M. Leewis, A. M. de Jong, L. J. van IJzendoorn, D. J. Broer, *J. Appl. Phys.* **2004**, *95*, 8352.
[14] T. Boussie, M. Devenney, *Eur. Pat. 1160262 A1*, **2001**.
[15] It should be noted that collecting more data points in the photoinitiator range 0–2 % would provide better insight into the optimum concentration for the given experimental conditions.
[16] D. Trimbach, K. Feldman, N. D. Spencer, D. J. Broer, C. W. M. Bastiaansen, *Langmuir* **2003**, *19*, 10 957.

Bioassisted Room-Temperature Immobilization and Mineralization of Zinc Oxide—The Structural Ordering of ZnO Nanoparticles into a Flower-Type Morphology**

By *Mitsuo Umetsu*, *Masamichi Mizuta*, *Kouhei Tsumoto*, *Satoshi Ohara*, *Seiichi Takami*, *Hideki Watanabe*, *Izumi Kumagai*, and *Tadafumi Adschiri**

Recent advances in biotechnology enable us to identify peptides with an affinity for non-biological materials and, in particular, those that mediate the mineralization of inorganic matter. The use of functional peptides is attracting immense interest in the development of bottom–up fabrication procedures of nanometer-scale devices. In biological systems, proteins such as silicatein,[1] silaffins,[2,3] and ferritin[4,5] cause the deposition of inorganic matter inside or around the cell where the nucleation and growth of these materials is controlled. These proteins are being utilized in vitro for the creation of nanostructured materials.[6–8] Recently, artificial peptides with an affinity for non-biological inorganic materials have been discovered by means of a combinatorial library approach,[9,10] and these peptides are known to have the potential for mineralization. For example, peptides with an affinity for metals and semiconductors, such as gold, silver, silica, zinc sulfide, and cadmium selenide, can be used to synthesize crystalline nano- to micrometer-sized metal particles.[11–15]

Zinc oxide, a semiconductor with a large direct bandgap, possesses unique optical, acoustic, and electronic properties. ZnO is one of the most widely studied metal oxides for use in solar cells,[16] sensors,[17] ultraviolet nanolasers,[18] and blue-light-emitting diodes (LEDs).[19] This wide variety of applications requires the fabrication of morphologically and functionally distinct ZnO nanostructures. Among the various methods of ZnO synthesis, wet-chemical approaches carried

[*] Prof. T. Adschiri, Dr. M. Umetsu, M. Mizuta, Dr. S. Ohara, Dr. S. Takami
Institute of Multidisciplinary Research for Advanced Materials
Tohoku University
2-1-1, Katahira, Aoba-ku, Sendai 980-8577 (Japan)
E-mail: ajiri@tagen.tohoku.ac.jp
Dr. K. Tsumoto, Dr. H. Watanabe, Prof. I. Kumagai
Department of Biomolecular Engineering
Graduate School of Engineering
Tohoku University
Aobayama 07, Aoba-ku, Sendai 980-8579 (Japan)

[**] This work was supported by a Scientific Research Grant from the Ministry of Education, Science, Sports, and Culture of Japan (MU, IK, and TA) and by the Industrial Technology Research Grant Program in '05 from New Energy and Industrial Technology Development Organization (NEDO) of Japan (MU). This research was also partly supported by the HEIWA NAKAJIMA foundation (TA) and by a Grant-in-Aid for the COE project, Giant Molecules and Complex Systems, 2002.

 DOI: 10.1002/adma.200500863